



Subsidence Performance of the Bioactive Glass-Ceramic ($\text{CaO-SiO}_2\text{-P}_2\text{O}_5\text{-B}_2\text{O}_3$) Spacer in Terms of Modulus of Elasticity and Contact Area: Mechanical Test and Finite Element Analysis

Myoung Lae Jo^{1,2}, Dong Min Son¹, Dong Ah Shin³, Bong Ju Moon⁴, Baek Hyun Kim¹, Kyung Hyun Kim⁵

■ **OBJECTIVE:** The objective of this study is to evaluate the subsidence performance of a bioactive glass-ceramic ($\text{CaO-SiO}_2\text{-P}_2\text{O}_5\text{-B}_2\text{O}_3$) spacer in terms of its modulus of elasticity and contact area using mechanical tests and finite element analysis.

■ **METHODS:** Three spacer three-dimensional models (Polyether ether ketone [PEEK]-C: PEEK spacer with a small contact area; PEEK-NF: PEEK spacer with a large contact area; and Bioactive glass [BGS]-NF: bioactive glass-ceramic spacer with a large contact area) are constructed and placed between bone blocks for compression analysis. The stress distribution, peak von Mises stress, and reaction force generated in the bone block are predicted by applying a compressive load. Subsidence tests are conducted for three spacer models in accordance with ASTM F2267. Three types of blocks measuring 8, 10, and 15 pounds per cubic foot are used to account for the various bone qualities of patients. A statistical analysis of the results is conducted using a one-way Analysis of variance and post hoc analysis (Tukey's Honestly Significant Difference) by measuring the stiffness and yield load.

■ **RESULTS:** The stress distribution, peak von Mises stress, and reaction force predicted via the finite element analysis are the highest for PEEK-C, whereas they are similar for

PEEK-NF and BGS-NF. Results of mechanical tests show that the stiffness and yield load of PEEK-C are the lowest, whereas those of PEEK-NF and BGS-NF are similar.

■ **CONCLUSIONS:** The main factor affecting subsidence performance is the contact area. Therefore, bioactive glass-ceramic spacers exhibit a larger contact area and better subsidence performance than conventional spacers.

INTRODUCTION

Anterior cervical discectomy and fusion (ACDF) surgery has been widely performed as the standard treatment for degenerative cervical disc diseases since its introduction by Smith and Robinson in 1958.¹⁻³ Although autologous bone graft harvested from the iliac crest is used as the gold standard with regard to fusion rate and biomechanical support for ACDF,⁴ donor site morbidity such as pain and wound infection subsidence as well as graft resorption have been reported.⁵⁻⁷ Hence, various bone substitutes, including allografts and spacers with osteoinductive materials and ceramics, have been introduced and widely used. However these substitutes exhibit disadvantages such as spacer breakage, migration, and nonunion, thus resulting in delayed bone fusion or reoperation.⁸⁻¹⁰

Key words

- Anterior cervical discectomy and fusion (ACDF)
- Bioactive glass-ceramic($\text{CaO-SiO}_2\text{-P}_2\text{O}_5\text{-B}_2\text{O}_3$)
- Cervical spacer
- Contact area
- Finite element analysis
- Modulus of elasticity
- Subsidence

Abbreviations and Acronyms

ACDF: Anterior cervical discectomy and fusion
BGS: Bioactive glass
FEA: Finite element analysis
PVMS: Peak von mises stress
PEEK: Polyether ether ketone
PCF: Pounds per cubic foot

From the ¹CGBio Co. Ltd., Seoul; ²Department of Biomedical Engineering, Chungbuk National University, Cheongju; ³Department of Neurosurgery, Spine and Spinal Cord Institute, Severance Hospital, Yonsei University College of Medicine, Seoul; ⁴Department of Neurosurgery, Chonnam National University Hospital and Medical School, Research Institute of Medical Sciences, Gwangju; and ⁵Department of Neurosurgery, Spine and Spinal Cord Institute, Gangnam Severance Hospital, Yonsei University College of Medicine, Seoul, Republic of Korea

To whom correspondence should be addressed: Kyung Hyun Kim, M.D., Ph.D.
 [E-mail: NSKHK@yuhs.ac]

Myoung Lae Jo and Dong Min Son contributed equally to this work.

Citation: *World Neurosurg.* (2023) 180:e1-e10.




<https://doi.org/10.1016/j.wneu.2023.05.034>

Journal homepage: www.journals.elsevier.com/world-neurosurgery

Available online: www.sciencedirect.com

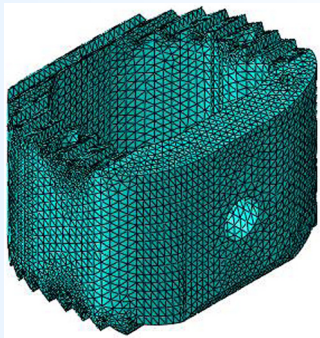
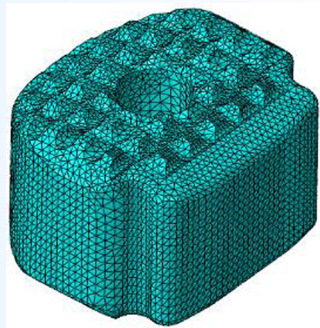
1878-8750/© 2023 The Authors. Published by Elsevier Inc. This is an open access article under the CC BY license (<http://creativecommons.org/licenses/by/4.0/>).

Table 1. Cervical Spacer Models (PEEK-C, PEEK-NF, BGS-NF)

Model	PEEK-C	PEEK-NF	BGS-NF
Image			
Size (W x L x H mm)	15 x 13 x 10	15 x 13 x 10	15 x 13 x 10
Contact area (mm ²)	89.75	171.58	171.58

PEEK, polyether ether ketone; BGS, bioactive glass.

Table 2. Finite Element Models (PEEK-C, PEEK-NF, BGS-NF)

Model	PEEK-C	PEEK-NF	BGS-NF
Image			
Number of node	1,306,664	1,202,613	
Number of element	918,007	849,225	
PEEK, polyether ether ketone; BGS, bioactive glass.			

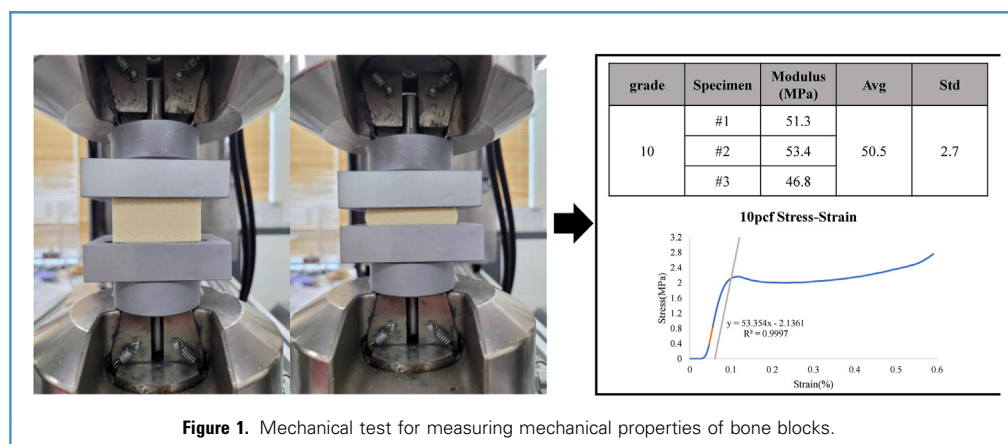


Figure 1. Mechanical test for measuring mechanical properties of bone blocks.

Over recent decades, several spacer materials have been developed, most notably titanium alloys and polyether ether ketone (PEEK) spacers. Titanium alloys are known for their high biocompatibility and can be directly fused with bone through surface treatment; however, they exhibit a high modulus of elasticity, thus resulting in a high rate of subsidence.¹¹⁻¹³ PEEK spacers have a modulus of elasticity similar to that of cortical bone; however, subsidence has been reported in these spacers.^{14,15}

A synthetic bioactive glass-ceramic spacer (NOVOMAX FUSION) was recently developed; it is fabricated using BGS-7($\text{CaO-SiO}_2\text{-P}_2\text{O}_5\text{-B}_2\text{O}_3$) to afford a large contact area and can be fused with bone tissue by forming a hydroxycarbonate apatite layer in body fluids, which results in faster osseointegration.¹⁶⁻¹⁸ In addition, it can prevent the breakage of implants as its mechanical strength is higher than that of conventional synthetic bone materials, titanium alloys, PEEK.¹⁹

This study is performed to evaluate the biomechanical safety of ceramic spacers in terms of subsidence in ADCF and to prove that

the main factor affecting subsidence is the contact area of the spacer, not the mechanical properties of the spacer material. The methods used in this study are finite element analysis (FEA) and mechanical tests.

METHODS

Finite Element Analysis FEA was performed to predict the factors affecting the material properties and contact area. Three models were constructed using different materials and contact areas. As a commercial product, the conventional PEEK spacer (PEEK-C) has a small contact area. The PEEK spacer (PEEK-NF) and bioactive glass-ceramic spacer (BGS-NF) were of the same shape as the large contact surface. These three models were designed to have the same dimensions (i.e., 15 mm wide, 13 mm long, and 10 mm high) using the SolidWorks 2020 software (SP5.0, Dassault Systems, France) (see Table 1).

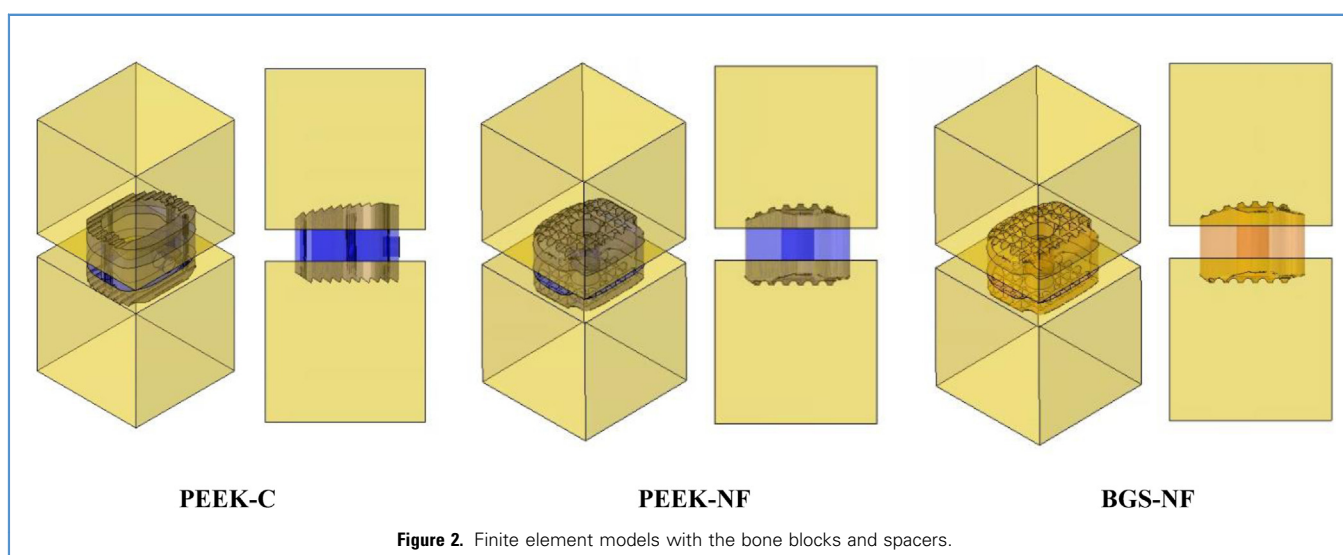


Figure 2. Finite element models with the bone blocks and spacers.

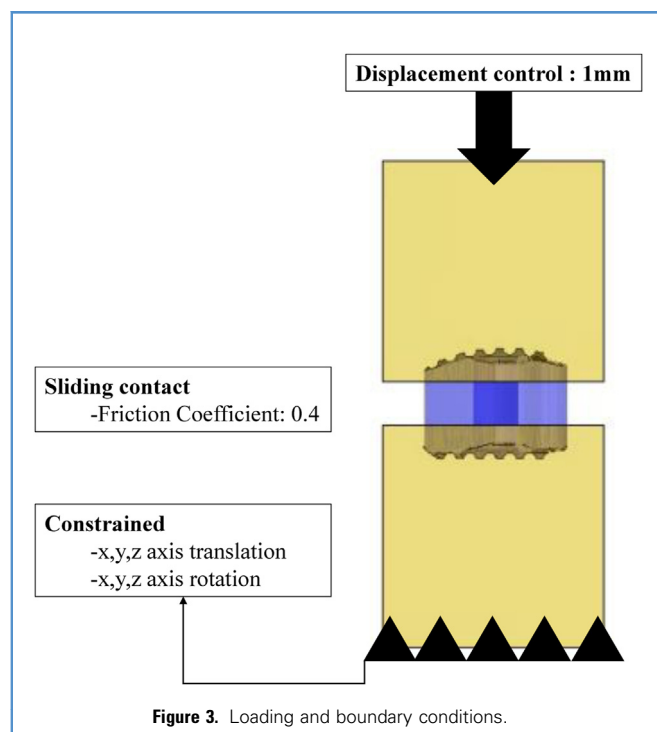


Figure 3. Loading and boundary conditions.

To construct the bone block model for the subsidence test in accordance with ASTM F2267, it was designed as a 20 mm × 20 mm × 20 mm cube using SolidWorks. The designed spacer and bone block models were imported into Abaqus (version 6.14; Dassault Systems, France), which is a FEA software, and constructed as finite element models. The mesh of the finite element model was composed of a tetrahedral mesh measuring 0.5 mm, and a quadratic mesh shape was selected to realize the curved shape of the spacer. The number of elements and nodes of each model are listed in Table 2.

To determine the mechanical properties of the bone block, a compression test was performed on a bone block measuring 10 pounds per cubic foot (PCF). A stress–strain curve was obtained via a compression test, and the nonlinear stress–strain curve and density (0.16 g/cc) values were input simultaneously in the bone block model (see Figure 1).²⁰ Linear properties were applied to PEEK (Young's modulus: 4 GPa; Poisson's ratio: 0.4)²¹ and BGS-

$$\text{Poisson's Ratio} = [1 - 2(v_s/v_l)^2] / [1 - (v_s/v_l)^2]$$

$$\text{Young's Modulus of Elasticity} = [\rho v_s^2 (3v_l^2 - 4v_s^2)] / (v_l^2 - v_s^2)$$

v_s = ultrasonic transverse velocity; v_l = ultrasonic longitudinal velocity;

$$\rho = \text{density} \quad (1)$$

7 (Young's modulus: 121 GPa; Poisson's ratio: 0.28). The mechanical properties of BGS-7 were determined via ultrasonic velocity measurements (Equation 1).²²

Table 3. Classification of Bone Blocks According to Density

PCF	Density (g/cc)	Classification
8	0.13	Low bone mass
10	0.16	Normal bone
15	0.24	High bone mass

Each spacer model was placed between two bone block models with an intradiscal height (distance between blocks) of 4 mm (in accordance with ASTM F2267) to achieve the same conditions as the actual test.²³ Furthermore, this would allow the surface of the bone block and the spacer to be in complete contact (see Figure 2).

A sliding contact with a friction coefficient of 0.4 was applied as the boundary condition between the spacer and the block.²⁴

The lower block was constrained to avoid movement for all degrees of freedom, and a displacement of 1 mm was applied to the upper block in the displacement-control compression direction (Figure 3). Subsequently, the stress distribution, the von Mises stress and strain occurring in the bone block, and the reaction force of the entire structure were predicted for result analysis.

Mechanical Test

Three types of spacer models created using the SolidWorks software were used to prepare the specimens for mechanical testing. For the bone block, three blocks measuring 8, 10, and 15 PCF were cut to the same size as the finite element model (20 mm × 20 mm × 20 mm) to account for the various bone qualities of each patient (see Table 3).^{20,25}

A stainless steel jig that can be inserted with a block was fixed to a Servohydraulic MTS (MTS 858 Bionix Testing Machine). Each spacer was placed between the two bone blocks and fixed on a testing machine. In accordance with the international test standard ASTM F2267, an axial compressive load was applied at a load speed of 0.1 mm/s until a displacement point of approximately 5 mm was reached. Data were obtained at a speed of 50 mm/s (see Figure 4).²³

After the test was completed, a load–displacement graph was obtained using the displacement and load values for each section. The yield load and stiffness of each implant were measured and the results were compared. For comparison, the validity of the difference in results was statistically analyzed using one-way Analysis of variance and post hoc analysis (Tukey's Honestly Significant Difference). In addition, because BGS-NF is an approved medical device, its Kp value was obtained for comparison with those of the Food and Drug Administration-approved products reported in the literature.²⁶

RESULTS

Finite Element Analysis

The peak von Mises stress (PVMS) and stress distribution in the bone block for the linear section were verified. When the displacement was applied in the compression direction, the stress up to the linear strain section was predicted. The PVMS and

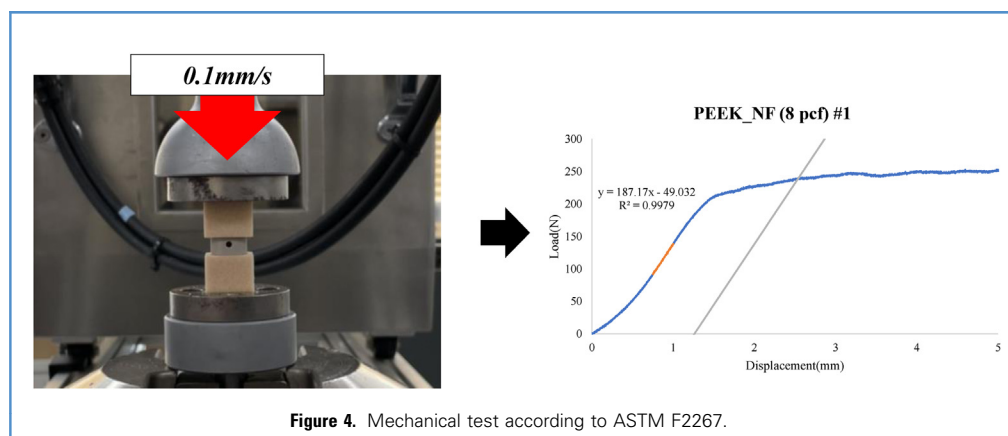


Figure 4. Mechanical test according to ASTM F2267.

reaction force on PEEK-C were predicted to be approximately 1.5 to 2 times higher than those on PEEK-NF and BGS-NF (Table 4). Similar results were predicted for the stresses in PEEK-NF and BGS-NF. Results of stress distribution prediction indicated that high stresses were more widely distributed in PEEK-C than in the other spacers (Figure 5). In addition, PEEK-NF and BGS-NF showed similar stress distributions despite their different materials.

Mechanical Test

The stiffness and yield load were obtained for each bone block.

The stiffness was the lowest for PEEK-C in all blocks. In the 8 and 10 PCF blocks, the stiffness of PEEK-NF was the highest, and in the 15 PCF block, the stiffness of BGS-NF was the highest. In the 8 PCF and 15 PCF blocks, a statistically significant difference was observed in terms of the contact area ($P < 0.01$), whereas no statistically significant difference was observed when material difference was indicated ($P > 0.01$). Among the 10 PCF blocks, significant difference was indicated ($P < 0.01$) (Figure 6).

Table 4. Finite Element Analysis Results of the Bone Blocks Combined with Spacers (PVMS, Reaction Force)

Strain	0.01	0.02	0.035	0.0575	0.0913	0.1
PVMS (MPa)						
PEEK-C	0.43	0.86	1.51	2.16	2.16	2.16
PEEK-NF	0.35	0.5	0.88	1.45	2.15	2.14
BGS-NF	0.35	0.52	0.9	1.48	2.15	2.14
Reaction force (N)						
PEEK-C	4.61	16.15	42.15	92.48	138.33	205.6
PEEK-NF	4.78	16.73	47.87	95.89	167.79	274.35
BGS-NF	4.81	16.85	48.21	96.58	168.94	276.07

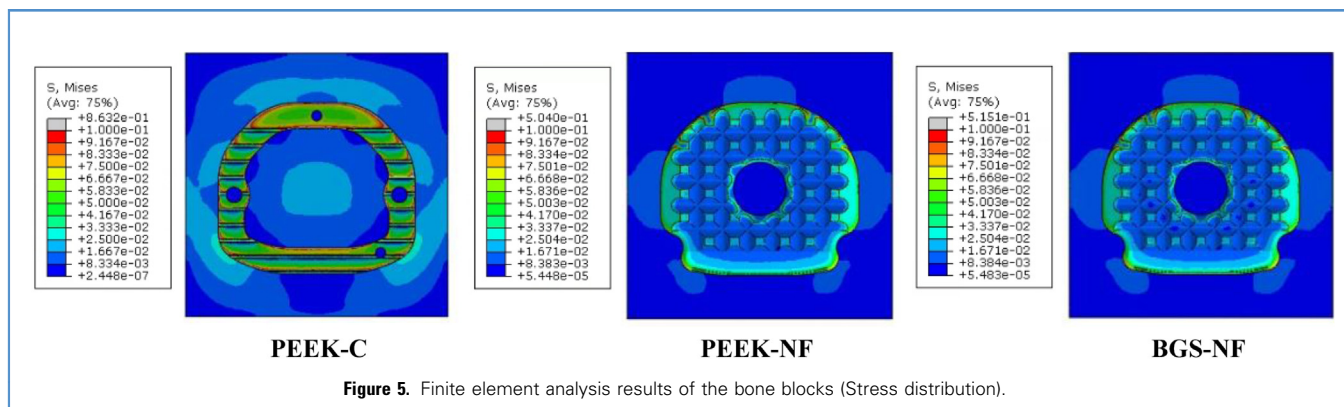
PVMS, peak von mises stress; PEEK, polyether ether ketone; BGS, bioactive glass.

The yield load was the lowest for PEEK-C and the highest for BGS-NF in all blocks. In the 8 and 15 PCF blocks, statistically significant difference was indicated in terms of the contact area ($P < 0.01$), whereas no statistically significant difference was observed when material difference was indicated ($P > 0.01$). Among the 10 PCF blocks, significant difference was indicated ($P < 0.01$) (Figure 7).

DISCUSSION

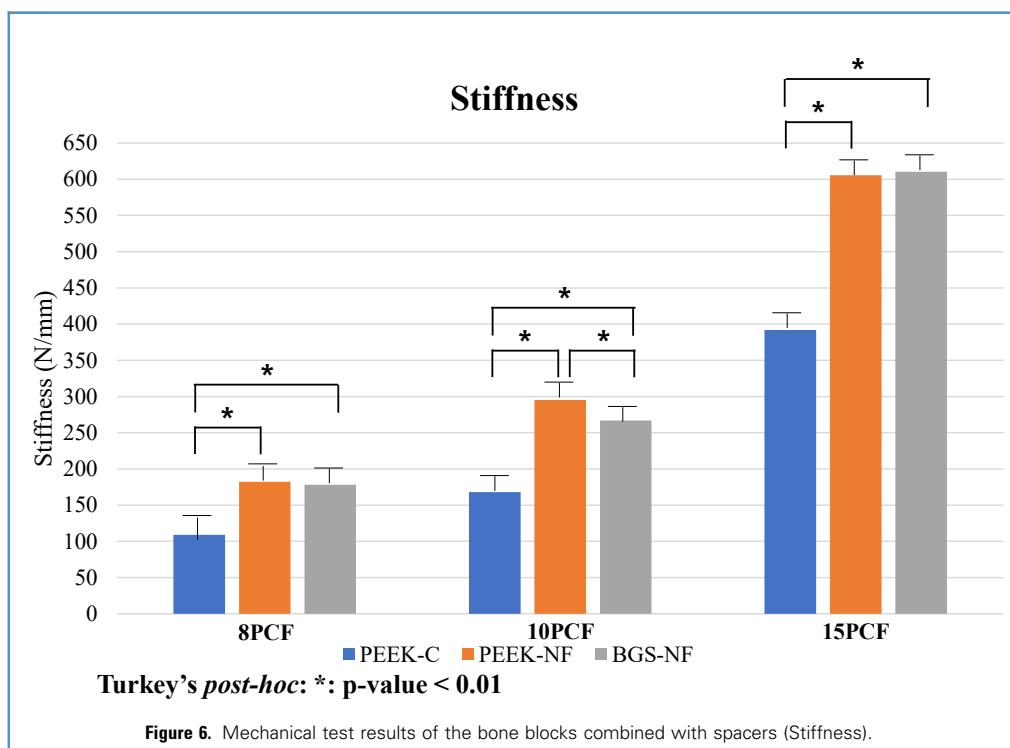
In this study, we investigated the safety of a bioactive glass-ceramic spacer fabricated using BGS-7 against subsidence. The ceramic spacer exhibited osseointegration on the surface; therefore, it does not require a large volume of bone graft (unlike the conventional cervical spacer) and is designed to allow a wide contact surface with the endplate. However, because BGS-7 exhibits high mechanical strength and modulus of elasticity owing to the characteristics of ceramics, the subsidence rate may be high. Therefore, safety was evaluated in terms of the materials and contact surface. The comparative material was PEEK, which has a modulus of elasticity similar to that of bone and has been actively used as a spacer material for ACDF since the early 2000s. The causes of subsidence by the spacer are (1) stress shielding due to the difference in the modulus of elasticity between the bone and spacer and (2) stress due to the contact area of the spacer. However, stress shielding is not a significant factor as no structure other than the spacer exists to transfer the load before interbody fusion.^{27,28} Although the PEEK spacer has a modulus of elasticity similar to that of the endplate,^{29,30} subsidence by PEEK spacers has been reported.^{14,15} Therefore, whether the modulus of elasticity is the main factor contributing to biomechanical subsidence remains unclear; as such, contact stress as the main factor should be considered. To reduce the stress on the contact surface, the spacer must be designed to have a wide contact surface; however, the wider the contact surface, the smaller is the space available for implanting the bone graft material. Hence, the spacer allows bony fusion directly on the surface.

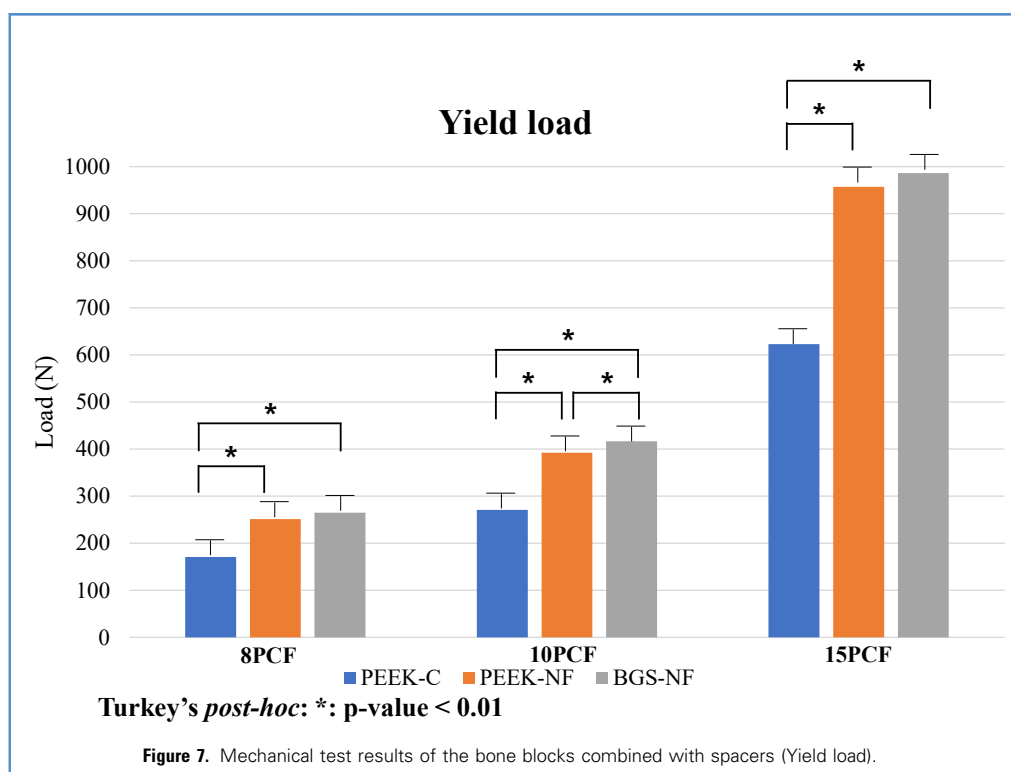
In this study, a conventional PEEK spacer (PEEK-C) and two spacers (PEEK-NF and BGS-NF) with the same design but



different materials were investigated to elucidate the effects of contact area and modulus of elasticity on subsidence. FEA and the ASTM I test method were used for evaluation. First, FEA was performed to predict the differences among the three models prior to conducting the ASTM F2267 test. To increase the reliability of the results, the stress–strain curve obtained via the compression test of 10 PCF polyurethane bone blocks with normal bone density was applied to the FEA. The highest PVMS and stress concentrations were predicted for PEEK-C, which features a small contact area with the endplate. Meanwhile, the PVMS and stress distributions were similar for PEEK-NF and BGS-NF.

After performing FEA, we conducted subsidence tests on the 8, 10, and 15 PCF test blocks. The 8 PCF block exhibited a density and mechanical properties that correspond to low bone density, whereas the 15 PCF block demonstrated high-quality bone properties, based on the subsidence test standard ASTM F2267 for the approval of spinal spacers by various authorities, including the Food and Drug Administration.^{20,24,25} We may consider using a cadaver to implement a clinical environment; however, increasing the number of test specimens will be difficult owing to limited donors. In addition, each donor exhibits wide variation in terms of bone quality. Therefore, to obtain accurate results, multiple specimens





should not be tested on the same cervical vertebral body. However, reliable results can be obtained because polyurethane test blocks have standardized mechanical properties.³¹

The test results confirmed that the stiffness and yield load decreased with the grade of the test block for all three models. When comparing each model, the general PEEK-C indicated significantly lower ($P < 0.01$) stiffness and yield loads than the other two models for test blocks of all grades. By contrast, the PEEK-NF and BGS-NF models showed similar values for the 8 and 15 PCF blocks ($P > 0.01$), whereas no significant difference

was indicated for the 10 PCF block ($P < 0.01$). This difference is attributed to the mechanical properties of the spacer on the test. In general, the test results confirmed that, although the modulus of elasticity of BGS-7 was much higher than that of PEEK, it did not affect subsidence significantly, and the contact area between the endplate and spacer was the main factor affecting subsidence.

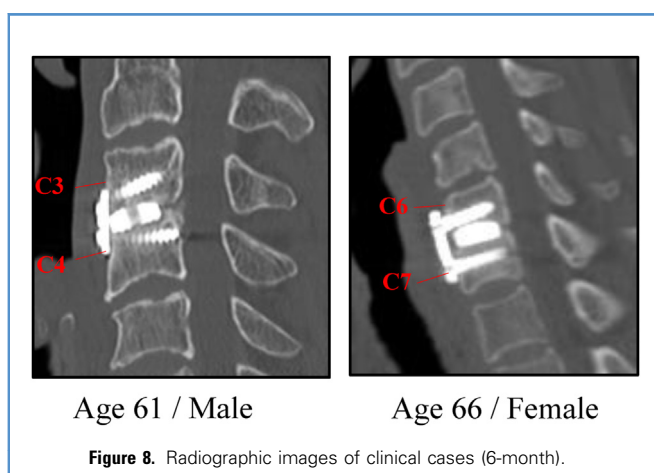
In this study, subsidence performance was measured based on K_s , which is the result of the entire system with both the test blocks and spacer. The stiffness value recommended by authorities responsible for medical devices is K_p , which is converted from Equation 2, where K_p represents the subsidence performance of the test block. The actual commercialized medical device is BGS-NF, which converts K_p at 15 PCF into K_p . Based on a comparison of the subsidence performance with those of cervical spinal spacers registered in the United States, the BGS-NF belongs to the top 5%–25%.³⁰

$$K_p = K_s K_d / K_d - K_s$$

K_d = stiffness of the intervertebral body fusion device

K_s = stiffness of the system (2)

In a retrospective study by Kim³² using allospacer-shaped spacers fabricated using BGS-7, no subsidence (0/32) exceeding 3 mm occurred for 2 years after surgery. Park³³ reported that no subsidence (0/26) occurred in the results of a 12-month study.



Subsidence occurred in approximately 12.5% (4/32) of Kim's spacers in the 2-year follow-up,³⁴ although it was significantly lower than that reported in the allograft control group (52.5%). These clinical results are consistent with those of the results of biomechanical study conducted in the present study. In addition, based on the radiographic images of the clinical cases, bone fusion progressed without subsidence at 6 months (Figure 8). The clinical study was conducted once the analysis was completed.

A limitation of this study is that safety was predicted based on only mechanical performance evaluation; hence, further clinical studies are required. In addition, a comparative study using a titanium cervical spacer fabricated via additive manufacturing, which enables a mesh-shaped surface and a wide contact area, is necessary.

CONCLUSIONS

A bioactive glass-ceramic spacer featuring a large contact area with the endplate in ACDF was designed in this study. Our results indicated its good subsidence performance. Additionally, its good mechanical properties did not affect subsidence performance, unlike PEEK.

CRediT AUTHORSHIP CONTRIBUTION STATEMENT

Myoung Lae Jo: Conceptualization, Validation, Formal analysis, Investigation, Writing – original draft. **Dong Min Son:** Methodology, Validation, Formal analysis, Data curation, Writing – original draft. **Dong Ah Shin:** Investigation, Writing – review & editing. **Bong Ju Moon:** Investigation, Writing – review & editing. **Baek Hyun Kim:** Methodology, Resources. **Kyung Hyun Kim:** Investigation, Writing – review & editing, Supervision, Project administration.

REFERENCES

- Smith GW, Robinson RA. The treatment of certain cervicospine disorders by anterior removal of the intervertebral disc and interbody fusion. *J Bone Joint Surg Am.* 1958;40-A:607-624.
- Bohlman HH, Emery SE, Goodfellow DB, Jones PK. Robinson anterior cervical discectomy and arthrodesis for cervical radiculopathy. Long-term follow-up of one hundred and twenty-two patients. *J Bone Joint Surg Am.* 1993;75:1298-1307.
- Geer CP, Papadopoulos SM. The argument for single-level anterior cervical discectomy and fusion with anterior plate fixation. *Clin Neurosurg.* 1999;45:25-29 [discussion: 21].
- Ryken TC, Heary RF, Matz PG, et al. Techniques for cervical interbody grafting. *J Neurosurg Spine.* 2009;11:203-220.
- Zdeblick TA, Hughes SS, Riew KD, Bohlman HH. Failed anterior cervical discectomy and arthrodesis. Analysis and treatment of thirty-five patients. *J Bone Joint Surg Am.* 1997;79:523-532.
- Eysel P, Fürderer S, Rompe JD, Zöllner J. Initial instability of different cages for fusion of the cervical spine. *Zentralbl Neurochir.* 2000;61:171-176.
- McAfee PC. Interbody fusion cages in reconstructive operations on the spine. *J Bone Joint Surg Am.* 1999;81:859-880.
- Miller LE, Block JE. Safety and effectiveness of bone allografts in anterior cervical discectomy and fusion surgery. *Spine (Phila Pa 1976).* 2011;36:2045-2050.
- Samartzis D, Shen FH, Matthews DK, Yoon ST, Goldberg EJ, An HS. Comparison of allograft to autograft in multilevel anterior cervical discectomy and fusion with rigid plate fixation. *Spine J.* 2003;13:451-459.
- Yue WM, Brodner W, Highland TR. Long-term results after anterior cervical discectomy and fusion with allograft and plating: a 5- to 11-year radiologic and clinical follow-up study. *Spine (Phila Pa 1976).* 2005;30:2138-2144.
- Chen Y, Chen D, Guo Y, et al. Subsidence of titanium mesh cage: a study based on 300 cases. *J Spinal Disord Tech.* 2008;21:489-492.
- Chou YC, Chen DC, Hsieh WA, et al. Efficacy of anterior cervical fusion: comparison of titanium cages, polyetheretherketone (PEEK) cages and autogenous bone grafts. *J Clin Neurosci.* 2008;15:1240-1245.
- Niu CC, Liao JC, Chen WJ, Chen LH. Outcomes of interbody fusion cages used in 1 and 2-levels anterior cervical discectomy and fusion: titanium cages versus polyetheretherketone (PEEK) cages. *J Spinal Disord Tech.* 2010;23:310-316.
- Yang JJ, Yu CH, Chang BS, Yeom JS, Lee JH, Lee CK. Subsidence and nonunion after anterior cervical interbody fusion using a stand-alone polyetheretherketone (PEEK) cage. *Clin Orthop Surg.* 2011;3:16-23.
- Le TV, Baaj AA, Dakwar E, et al. Subsidence of polyetheretherketone intervertebral cages in minimally invasive lateral retroperitoneal transposas lumbar interbody fusion. *Spine.* 2012;37:1268-1273.
- Lee JH, Seo JH, Lee KM, Ryu HS, Baek HR. Fabrication and evaluation of osteoblastic differentiation of human mesenchymal stem cells on novel CaO-SiO₂-P₂O₅-B₂O₃ glass-ceramics. *Artif Organs.* 2013;37:637-647.
- Lee JH, Lee KM, Jang SJ, Lee HS, Baek HR. Effects of bisphosphonate-treated bioactive ceramic grafts for the proliferation and osteoblastic differentiation of human bone marrow mesenchymal stem cells. *Tissue Eng Regen Med.* 2011;8:69-77.
- Lee JH, Jeung UO, Jeon DH, Chang BS, Lee CK. Quantitative comparison of novel CaO-SiO₂-P₂O₅-B₂O₃ glass-ceramics (BGS-7) with hydroxyapatite as bone graft extender in rabbit ilium. *Tissue Eng Regen Med.* 2010;7:540-547.
- Koo KH, Hwang CJ, Lee JH, Chang BS, Lee CK. Treatment of bone defects in rabbit tibiae using CaO-SiO₂-P₂O₅-B₂O₃ bioactive ceramics: radiological, biomechanical, and histological evaluation. *Tissue Eng Regen Med.* 2009;6:811-818.
- Nagaraja S, Palepu V. Comparisons of anterior plate screw pullout strength between polyurethane foams and thoracolumbar cadaveric vertebrae. *J Biomech Eng.* 2016;138. <https://doi.org/10.1115/1.4034427>.
- McIntire BJ, Bal BS, Rahaman MN, Chevalier J, Pezzotti G. Ceramics and ceramic coatings in orthopaedics. *J Eur Ceram Soc.* 2015;35:4327-4369.
- Standard Practice for Measuring Ultrasonic Velocity in Material. ASTM E494-15. ASTM International; 2015.
- Standard Test Method for Measuring Load Induced Subsidence of Intervertebral Body Fusion Device under Static Axial Compression. ASTM F2267-04. ASTM International; 2004.
- Adam C, Pearcy M, McCombe P. Stress analysis of interbody fusion-finite element modelling of intervertebral implant and vertebral body. *Clin Biomech.* 2003;18:265-272.
- ACR practice guideline for the performance of quantitative computed tomography (QCT) bone densitometry. Chicago, IL: American College of Radiology; 2008.
- Peck JH, Sing DC, Nagaraja S, Peck DG, Lotz JC, Dmitriev AE. Mechanical performance of cervical intervertebral body fusion devices: a systematic analysis of data submitted to the Food and Drug Administration. *J Biomech.* 2017;54:26-32.
- Naghavi SA, Lin C, Sun C, et al. Stress shielding and bone resorption of press-fit polyether-etherketone (PEEK) hip prosthesis: a Sawbone model study. *Polymers.* 2022;14:4600.
- Huiskes R, Weinans H, van Rietbergen B, et al. The relationship between stress shielding and bone resorption around total hip stems and the effects of flexible material around total hip

- stems and the effects of flexible materials. *Clin Orthop Relat Res.* 1992;124-134.
29. Wu Y, Loaiza J, Banerji R, Blouin O, Morgan E. Structure-function relationships of the human vertebral endplate. *JOR Spine.* 2021;4:e1170.
 30. Polyetheretherketone (PEEK) Polymers for Surgical Implant Applications. ASTM F2026-17. ASTM International; 2017.
 31. Standard Specification for Rigid Polyurethane Foam for Use as a Standard Material for Testing Orthopaedic Devices and Instruments. ASTM F1839-08. ASTM International; 2021.
 32. Kim HC, Oh JK, Kim DS, et al. Comparison of the effectiveness and safety of bioactive glass ceramic to allograft bone for anterior cervical discectomy and fusion with anterior plate fixation. *Neurosurg Rev.* 2020;43:1423-1430.
 33. Park S, Lee DH, Seo J, et al. Feasibility of CaO-SiO₂-P₂O₅-B₂O₃ bioactive glass ceramic cage in anterior cervical discectomy and fusion. *World Neurosurg.* 2020;141:e358-e366.
 34. Kim SH, Cho PG, Kwack K, Kim SH. Bioactive glass-ceramic (NOVOMAX®) spacer for anterior cervical discectomy and fusion: a minimum 2-year follow-up study. *Nerve.* 2020;6:57-65.

Conflict of interest statement: This work was supported by the Korea Medical Device Development Fund grant funded by the Korea government (the Ministry of Science and ICT, the Ministry of Trade, Industry and Energy, the Ministry of Health & Welfare, the Ministry of Food and Drug Safety) (Project Number: 1711174273, RS-2020-KD000253)
Received 7 January 2023; accepted 9 May 2023

Citation: *World Neurosurg.* (2023) 180:e1-e10.
<https://doi.org/10.1016/j.wneu.2023.05.034>

Journal homepage: www.journals.elsevier.com/world-neurosurgery

Available online: www.sciencedirect.com

1878-8750/© 2023 The Authors. Published by Elsevier Inc.
This is an open access article under the CC BY license (<http://creativecommons.org/licenses/by/4.0/>).